Communications

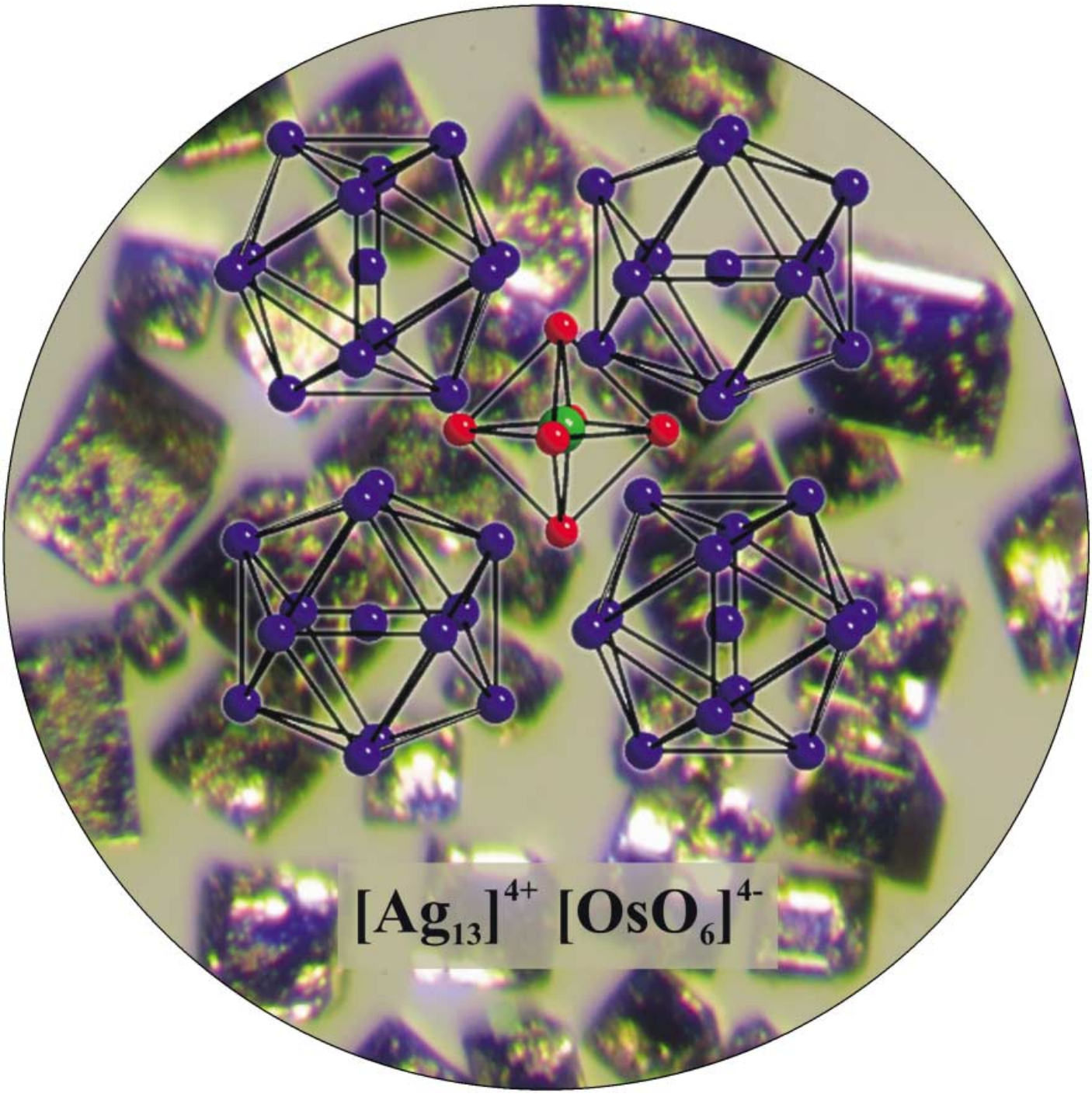

The $Ag_{13}OsO_6$ complex contains isolated Ag_{13}^{4+} icosahedral clusters in which the central silver ion has the distinction of being bonded solely to other silver ions. This unique character, and the electronic structure of the complex, is described by M. Jansen et al. on the following pages.

DOI: 10.1002/anie.200351740

Subvalent Ternary Silver Oxide

$Ag_{13}OsO_6$: A Silver Oxide with Interconnected Icosahedral Ag_{13}^{4+} Clusters and Dispersed $[OsO_6]^{4-}$ Octahedra**

*Sascha Ahlert, Wilhelm Klein, Ove Jepsen, Olle Gunnarsson, Ole Krogh Andersen, and Martin Jansen**

It has become possible to synthesize ternary silver oxides routinely by reacting the appropriate binary oxides in the solid state under oxygen pressure.[1] Recent systematic investigations have revealed that early, rare observations of unusually short silver–silver separations in oxides were not exceptions, but manifestations of a general feature of the chemistry of silver.[2–4] From our broad basis of experimental data the following picture now emerges: In oxides with high silver contents, silver atoms tend to cluster forming partial structures that are topologically reminiscent of elemental silver. These structures seem to be associated with specific physical properties.[5–7] Weak Ag^+–Ag^+ bonding therefore seems to exist, which indicates that monovalent silver (d^{10} configuration) can no longer be regarded as a closed-shell ion. As another consequence, the aggregates of monovalent silver ions provide empty 5s bands close to the Fermi level that should readily accommodate additional electrons, thus generating silver atoms in a valence state between 0 and +1. Based on such considerations, one would expect silver to be inclined to form subvalent compounds. In the past only singular cases like Ag_2F[8] were reported and, hence, considered as curiosities, but the number of cases is now steadily growing. Empty Ag_6^{4+} octahedra, as found in Ag_3O,[9] Ag_5SiO_4,[10] Ag_5GeO_4[11,12] and $Ag_6Ge_{10}P_{12}$[13] seem to prevail, while slabs of edge-sharing octahedra whose Ag centers have, on average, a charge of $+^1/_2$ have been found in Ag_2F[8] and Ag_2NiO_2.[14] In all known subvalent silver compounds, each silver atom has at least one oxygen atom as nearest neighbor. Here we describe a new subvalent ternary silver oxide, $Ag_{13}OsO_6$, whose icosahedral silver cluster contains a central atom, which is exclusively coordinated to silver.

The title compound was discovered by chance in the course of a systematic exploration of the ternary system Ag/Os/O. Due to the volatility of OsO_4, the Ag/Os ratio of 13:1 occurred spontaneously when starting with reactant mixtures containing far lower shares of silver. By elaborating on the optimal synthesis conditions, we noticed that $Ag_{13}OsO_6$ forms readily, and that various reaction conditions apply. Two feasible routes are: 1) to start with mixtures of the elements in the presence of water as a mineraliser, and 2) to react silver(I) oxide and elemental osmium in the solid state. In both cases, an oxygen pressure of 0.1–0.2 kbar must be maintained during the reaction; water promotes crystal growth. Crystals of cubic shape with edge lengths of up to 0.5 mm, as well as single-phase microcrystalline powders were obtained. The samples show a silver-metallic luster, and are insensitive to air. In argon atmosphere at 300 °C, thermal degradation occurs due to the emission of osmium (via OsO_4) and of oxygen, as detected by mass spectroscopy, leaving elemental silver as the only residue. No other decomposition products (e.g., water or hydroxide) have been detected.

$Ag_{13}OsO_6$ consists of OsO_6 octahedra and Ag_{13} icosahedra arranged as in CsCl (Figure 1).[15] The icosahedra are aligned with their twofold axes along the cubic directions with alternating 90° rotations so that the primitive cell contains two icosahedra and two octahedra.

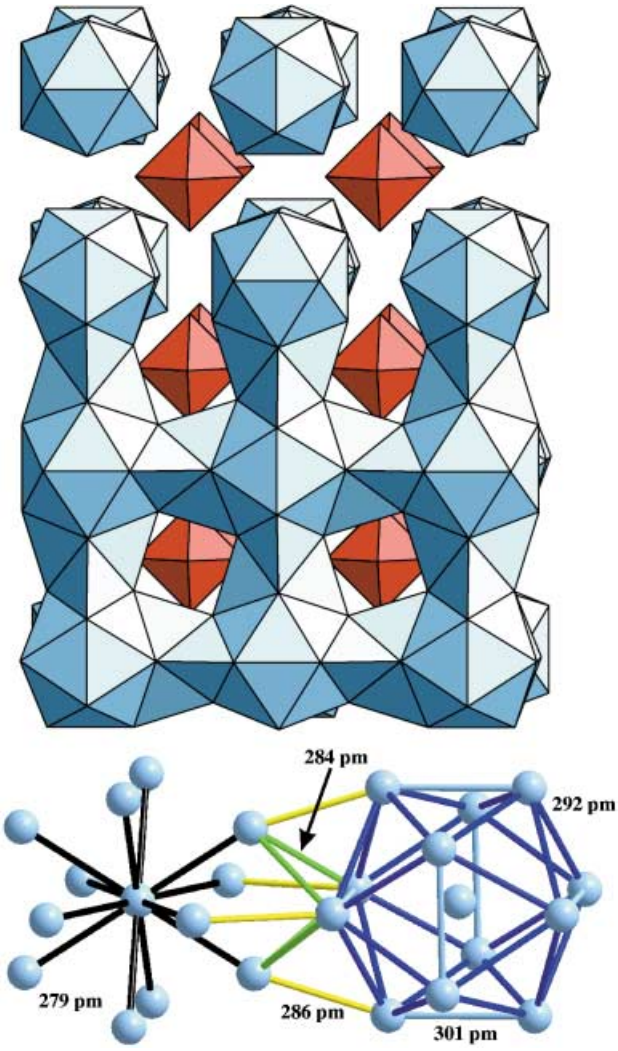

Figure 1. Crystal structure of $Ag_{13}OsO_6$. Triangular faces of oxygen and silver are shown in red and blue, respectively. In the upper part of the figure, the silver icosahedra have been disconnected. The lower part exhibits the different types of Ag–Ag interactions: central intracluster (black), short intracluster (dark blue), long intracluster (light blue), short intercluster (green), long intercluster (yellow).

[*] Prof. Dr. M. Jansen, S. Ahlert, Dr. W. Klein, Dr. O. Jepsen, Dr. O. Gunnarsson, Prof. Dr. O. K. Andersen
Max-Planck-Institut für Festkörperforschung
Heisenbergstrasse 1, 70567 Stuttgart (Germany)
Fax: (+49) 711-689-1502
E-mail: m.jansen@fkf.mpg.de

[**] The authors would like to thank the chemical service group, Eva Brücher, Gisela Siegle, and Dr. Reinhard K. Kremer for determining the electric and magnetic properties of the material.

  DOI: 10.1002/anie.200351740

All octahedra are parallel and aligned along the cubic directions. The shortest interatomic distance found in the structure is between Os and O. Its length (190 pm) does not allow a clear assignment of the osmium oxidation state, since for +6, +7, and +8, the effective Os radii differ by merely 3 pm; in the Os^{VII} compounds Na_5OsO_6[16] and Ba_2NaOsO_6[17] the Os–O distances are 190 and 187 pm, respectively. The octahedra are fairly close with a distance of merely 279 pm between the two apical oxygen atoms. The separation (246 pm) between the nearest silver atoms is significantly shorter than the sum of the Ag^+ and O^{2-} ionic radii (266 pm), although larger than commonly observed covalent Ag–O distances (200–230 pm). As seen in the lower part of the figure, these silver atoms form a square, which bisects the line between the two apical oxygen atoms of adjacent octahedra belonging to four different icosahedra. Although the OsO_6 octahedra are perfect, the site symmetry of their centers is not O_h, but only O. This is mostly due to a turn of the squares around the cubic axes, which leads to a loss of the mirror planes.

Whereas the number of crystallographically independent Os and O atoms is one, there are two kinds of silver atoms: Ag(1) at the centers of the icosahedra, and Ag(2) at the corners. As indicated at the bottom of Figure 1, Ag(1) has 12 nearest Ag(2) neighbors at a separation of 279 pm. This is closer than in elemental face-centered cubic (fcc) silver. Considering the fact that the distance along the 30 edges of a perfect icosahedron is 1.051 times the distance to the center, one finds that the average of the 42 near-neighbor distances in Ag_{13} is: $279\text{ pm} \times (12 + 30 \times 1.051)/42 = 289$ pm. This is exactly the nearest-neighbor distance in elemental Ag. In reality, the icosahedra are distorted with 24 short (291 pm) and six long (301 pm) edges. Nevertheless, their average is seen to be exactly 1.051 times 279 pm, so the conclusion remains that the average intracluster Ag–Ag separation in the icosahedron is as in elemental Ag. The symmetry around the center of the distorted icosahedron is T_h, a maximal subgroup of I_h. Of the 20 triangular faces, eight are equilateral with the short edges and 12 are isosceles with one long and two short edges. The long edges point along the cubic directions and alternate between, for example, the x and y directions.

The deviations from icosahedral symmetry are manifestations of strong intercluster bonding rather than of space-group requirements: We have seen that each Ag(2) center has six intracluster bonds (1×279 pm, 4×292 pm, 1×301 pm), but it has equally many intercluster bonds, and they are all short. The distance to the two oxygen atoms is 246 pm and the distance to the two nearest silver atoms in the square is 286 pm (yellow in Figure 1). The distance to the remaining two silver atoms is merely 284 pm, the shortest Ag(2)–Ag(2) distance in the structure (green). Keeping in mind that each Ag(2) center belongs to a long (301 pm) edge of its own icosahedron, it may be seen that these two short intercluster bonds are associated with the ends of a long edge perpendicular to their own long edge. The contact between two icosahedra thus consists of a perpendicular pair of long edges (light blue), joined at their ends by four short (284 pm) bonds (green).

$Ag_{13}OsO_6$ may be regarded as a nanoporous metal with the pores filled by octahedral oxoosmate anions. The building principle is similar to that of the intermetallic phases of type $NaZn_{13}$.[18]

$Ag_{13}OsO_6$ is a metallic conductor with a specific resistance of $\rho = 2.23 \cdot 10^{-4}\ \Omega\,\text{cm}$ at 298 K with a positive temperature coefficient of $0.77\ \mu\Omega\,\text{cm}\,\text{K}^{-1}$, and is diamagnetic. Neither the structural data nor the physical properties allow for an unambiguous determination of the oxidation state of Os. The diamagnetic behavior is compatible with the +8 state, but with strong spin–orbit coupling and ligand-field effects, ground states with reduced susceptibilities are possible also for hexa- or heptavalent osmium. In addition, structural reference data for Os–O bond lengths are rare, and not in all cases reliable or comparable. We have therefore performed density functional LMTO calculations[19] to gain an insight into the bonding and electronic properties.

Figure 2 shows the calculated electronic density of states (DOS), projected onto the sum of the orthonormal orbitals centered on Os, O, Ag(2), and Ag(1), respectively. Covalent interactions may be recognized as common DOS structures. The top and bottom panels display respectively the region of energies above (positive) and below (negative) the Fermi energy, taken as zero. Note that the vertical scale has been changed to accommodate more of the Ag 4d peak between −6.4 and −3.0 eV. A description of the calculated electronic structure begins with the strongest covalent interactions, that is, those on the OsO_6 octahedron. The hopping integral between the Os 6s orbital and the O 2p orbital of a_g symmetry is so strong that the bonding O 2p-like band is far below and the antibonding Os 6s-like band far above the Fermi level. For the purpose of counting, we may therefore say that there are no Os 6s-electrons, although the occupied bonding O 2p-like band has some Os 6s character. The peaks from the e_g bonding and antibonding bands are those extending from −7.4 to −6.9 eV and from 5.2 to 6.0 eV, respectively. Similarly, the t_{2g} bonding and antibonding bands are those extending respectively from −7.0 to −6.0 eV and from −0.2 to 1.0 eV. This means that the Os–O bonding states are occupied and the Os–O antibonding states are empty. This leaves 12 ($6 \times 3 - 1 - 2 - 3$) O 2p orbitals which do not bond to Os and which cause the broad peak between −3 and −1 eV. In conclusion, of the OsO_6 bands, all bonding and nonbonding O 2p-like bands are occupied, and all antibonding Os-like bands are empty. Therefore the charge state of the octahedron may be considered as $[OsO_6]^{4-}$, and that of the icosahedron as Ag_{13}^{4+}. Since the occupied bands have strong Os character, the notation $Os^{8+}O_6^{2-}$ should be avoided.[20]

The 0.2-eV filling of the antibonding t_{2g} band may be an artifact of the calculation, and a geometry optimization might place the Fermi level in the pseudo-gap. Here, the total DOS is 2.3 electrons per eV and per 2($Ag_{13}OsO_6$). Per Ag atom, this is 0.09, which is considerably smaller than the value $0.25\ \text{e}\,(\text{eV} \times \text{Ag})^{-1}$ in elemental fcc silver. This may explain the observed diamagnetism. The average DOS in the 5 eV region above the Fermi level has about the same value as in fcc Ag.

The positions and characters of the bonding and antibonding e_g and t_{2g} bands deviate considerably from what is obtained for an isolated OsO_6 octahedron. For instance, both

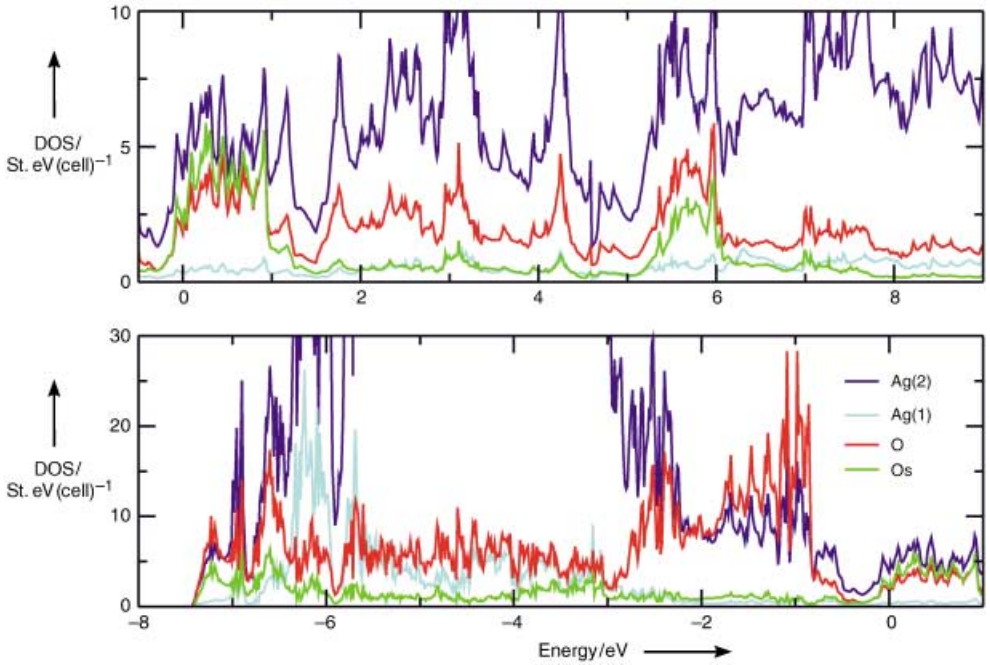

Figure 2. Electronic densities of states of $Ag_{13}OsO_6$ projected onto the sum of the orthonormal LMTOs centered on Os (green), O (red), Ag(1) (light blue), and Ag(2) (dark blue). The Fermi energy is taken to be zero.

e_g bands have more O than Os character. The reason for this is clearly seen in Figure 2, namely that Ag(2) character dominates the entire spectrum, including the e_g and t_{2g} peaks. Since silver reduces the symmetry from O_h to O, hybridization with the Ag(2) 4d, 5s, and 5p orbitals mixes odd, nonbonding O 2p character into the e_g and t_{2g} bands.

The silver 4d band extends from −6.4 to −3.0 eV, of which the part between −6.4 and −5.9 eV is the Ag(1) h_g (I_h) state. This 4d-band is more narrow and low-lying than in elemental fcc Ag, where it extends from −6.6 to −2.7 eV (in the local density approximation (LDA)). The difference is due to the Ag(2) 4d orbitals that form bonding and antibonding bands with the O 2p orbitals, which do not bond with Os. The corresponding DOS structures are visible between −3.0 and −0.5 eV, between 1.6 and 4.5 eV, and between 6.9 and 7.8 eV. The Ag(2) 5s and 5p projected densities of states (not explicitly shown) are similar to those in elemental Ag, where they exhibit sd and pd hybridization gaps and are fairly constant around the Fermi level. This is very different from the Os 6s projection, and from the Ag 5s and 5p projections in Ag oxides. Hence, in $Ag_{13}OsO_6$ it is mainly the Ag(2) 4d orbitals that are responsible for the interaction with O 2p, while the Ag 5s and 5p orbitals interact mainly with Ag orbitals.

This bonding situation can be expressed quantitatively by the covalent bond strengths (crystal orbital Hamiltonian populations (COHPs) integrated to the Fermi level)[21] calculated from the LMTO energies and eigenvectors. The strengths of the sticks between the atoms in Figure 3 have been assigned accordingly. With a strength of 3.4 eV, the 190 pm Os–O bond is the strongest in the structure. The oxygen atoms do not bind to each other (< 0.05 eV). Second strongest is the 246 pm Ag(2)–O bond (0.76 eV). Then

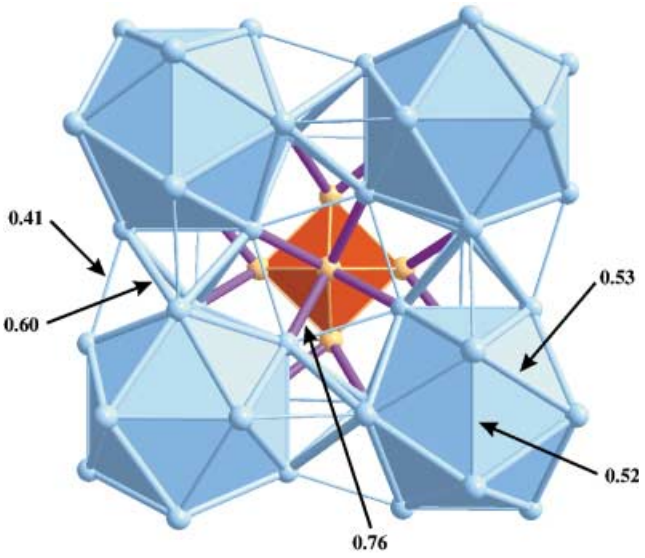

Figure 3. A more detailed view of a section of the structure shown in Figure 1. The sticks have been given a width roughly proportional to the calculated covalent bond strengths (COHPs integrated to the Fermi level). Numbers are in eV. The central Os–O (3.4 eV) and Ag(1)–Ag(2) (0.65 eV) bonds are not shown.

follows the 279 pm central Ag(1)–Ag(2) bond with a strength of 0.65 eV. The short (291 pm) and long (301 pm) Ag(2)–Ag(2) intracluster bonds are considerably weaker and nearly equal (0.52 and 0.53 eV). With a strength of 0.60 eV, the short (284 pm) intercluster bond connecting the ends of the perpendicular edges is the strongest Ag(2)–Ag(2) bond. Finally, the Ag(2)–Ag(2) intercluster bond along the 286 pm edge of a square is relatively weak (0.41 eV). Whereas the

average Ag–Ag intracluster separation is the same as in elemental fcc Ag, the bond strength of 0.64 eV in fcc Ag is reached only by the central Ag(1)–Ag(2) bond. This "deficit" is compensated by the strong bonding to oxygen atoms.

The band structure in the 4 eV region around the Fermi level is shown in Figure 4. The bands have been given a

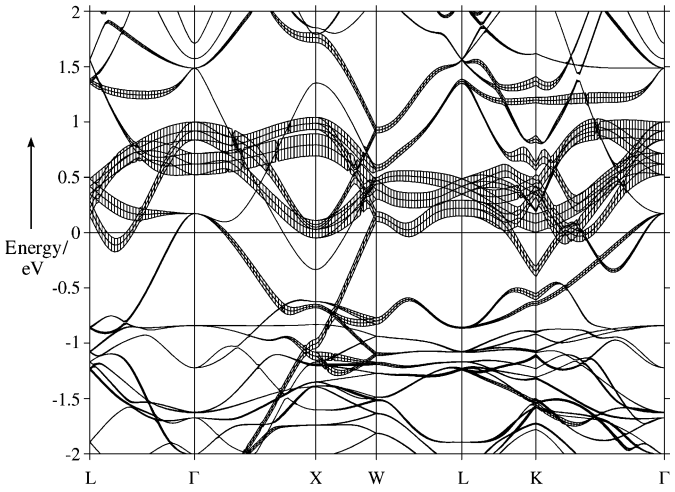

Figure 4. The band structure around the Fermi level (at 0 eV) of $Ag_{13}OsO_6$ along symmetry lines in the fcc Brillouin zone. The fatness of the bands is proportional to the Os t_{2g} character of the states.

degree of fatness that is proportional to their Os t_{2g} character. We see that the six antibonding t_{2g} bands disperse by $W \approx 1$ eV and that there is considerable additional mixing with the surrounding O 2p/Ag(2) bands. Simple estimates for the energy cost U of putting two electrons on the same OsO_6 octahedron give $U > W$. One would therefore expect interesting correlation effects in electron-doped systems where the t_{2g} band is partly occupied. If synthesized, $ZnAg_{12}OsO_6$ would be an obvious candidate.

Experimental Section

$Ag_{13}OsO_6$ was obtained by the solid-state reaction of ground mixtures of silver or silver oxide and osmium at elevated oxygen pressure. Due to the high volatility of the easily formed OsO_4 an excess of Os metal is necessary. Successful preparations have been run with Ag/Os molar ratios of 1:1 up to 5:1. In a typical experiment, $Ag_{13}OsO_6$ was obtained from a mixture of Ag (107.9 mg, 1 mmol) and Os (47.5 mg, 0.025 mmol) in a gold crucible at 15 MPa oxygen pressure and 300 °C for 2 days as a lustrous olive-green microcrystalline sample. To prepare silvery single crystals suitable for X-ray diffraction analysis, 1 mL H_2O was added as a mineralizer.

Received: April 24, 2003 [Z51740]
Published online: September 1, 2003

Keywords: cluster compounds · molecular orbital theory · osmium · silver · subvalent compounds

[1] C. Linke, M. Jansen, *Z. Anorg. Allg. Chem.* **1997**, *623*, 1441.
[2] M. Jansen, *Habilitationsschrift*, Universiät Gießen, **1978**.
[3] M. Jansen, *J. Less-Common Met.* **1980**, *76*, 285.
[4] M. Jansen, *Angew. Chem.* **1987**, *99*, 1136; *Angew. Chem. Int. Ed. Engl.* **1987**, *26*, 1098.
[5] C. Friebel, M. Jansen, *Z. Naturforsch. B* **1984**, *39*, 739.
[6] B. U. Köhler, M. Jansen, W. Weppner, *J. Solid State Chem.* **1985**, *57*, 227.
[7] P. Behrens, S. Aßmann, U. Bilow, C. Linke, M. Jansen, *Z. Anorg. Allg. Chem.* **1999**, *625*, 111.
[8] G. Argay, F. Naray-Szabo, *Acta Chim. Acad. Sci. Hung.* **1966**, 329.
[9] W. Beesk, P. G. Jones, H. Rumpel, E. Schwarzmann, G. M. Sheldrick, *J. Chem. Soc. Chem. Commun.* **1981**, 644.
[10] C. Linke, M. Jansen, *Inorg. Chem.* **1994**, *33*, 2614.
[11] M. Jansen, C. Linke, *Angew. Chem.* **1992**, *104*, 618; *Angew. Chem. Int. Ed. Engl.* **1992**, *31*, 653.
[12] M. Jansen, C. Linke, *Z. Anorg. Allg. Chem.* **1992**, *616*, 95.
[13] H. G. von Schnering, K. Häusler, *Rev. Chim. Miner.* **1976**, *13*, 71.
[14] M. Schreyer, M. Jansen, *Angew. Chem.* **2002**, *114*, 665; *Angew. Chem. Int. Ed.* **2002**, *41*, 643.
[15] Crystal data of $Ag_{13}OsO_6$: $0.1 \times 0.1 \times 0.1$ mm^3; cubic, $Fm\bar{3}c$, $a = 13.1712(5)$ Å; $V = 2284.95(15)$ Å^3; $Z = 8$, $\mu = 32.797$ mm^{-1}; $\rho_{calcd} = 9.817$ g cm^{-3}; Bruker AXS Smart CCD 1000, $Mo_{K\alpha}$, $\lambda = 0.71073$ Å; measurement range $3.09 = \theta = 34.96°$; $T = 293(2)$ K; 2367 independent reflections out of 7622 measured ($I > 2\sigma(I)$); solved by direct methods and subsequently refined by full-matrix, least-squares calculations based on F^2 (SHELXTL-V5.12); max./min. residual electron density $+1.60/-4.84$ e Å^{-3}, $R_1 = 0.0319$, $wR_2 = 0.0650$, GOF = 1.360. Further details on the crystal structure investigations may be obtained from the Fachinformationszentrum Karlsruhe, 76344 Eggenstein-Leopoldshafen, Germany (fax: (+49) 7247-808-666; e-mail: crysdata@fiz-karlsruhe.de), on quoting the depository number CSD-413193.
[16] T. Betz, R. Hoppe, *Z. Anorg. Allg. Chem.* **1985**, *524*, 17.
[17] K. E. Stitzer, M. D. Smith, H.-C. zur Loye, *Solid State Sci.* **2002**, *4*, 311.
[18] a) J. A. A. Ketelaar, *J. Chem. Phys.* **1937**, *5*, 668; b) E. Zintl, W. Hauke, *Nature* **1937**, *139*, 717; c) D. P. Shoemaker, R. E. March, F. J. Ewing, L. Pauling, *Acta Crystallogr.* **1952**, *5*, 637.
[19] The band-structure calculation was performed with the GGA Perdew–Wang density functional and the Stuttgart TB LMTO code. The sphere radii in pm were: 127 (Os), 110 (O), 99 (E), 157 (Ag(2)), and 160 (Ag(1)). The E spheres were placed at the faces of the octahedra, at the Wyckoff 64 g sites with $x = 0.1633$. The basis set included the Ag and Os s, p, and d LMTOs, the O p LMTOs, and the E s and p LMTOs. The O s and d partial waves were downfolded. Spin–orbit coupling was neglected in this scalar relativistic calculation; its inclusion would cause a t_{2g} band to split by $(3/2)\zeta_d \sim 0.3$ eV into a lower fourfold and an upper twofold degenerate band.
[20] The charges obtained from the occupations of our orthonormal LMTOs are: $Os^{+2.62}$, $O^{-0.86} = (O_6^{-0.26} + E_8^{-0.45})/6$, $Ag(1)^{-0.32}$, and $Ag(2)^{+0.24}$).
[21] R. Dronskowski, P. E. Blöchl, *J. Phys. Chem.* **1993**, *97*, 8617.

